Predicting Synchrony in a Simple Neuronal Network

Sachin S. Talathi and Pramod P. Khargonekar

1 Introduction

Human brain is comprised of hierarchically structured networks of neurons with feedforward and feedback connections across the hierarchy [17]. It has a remarkable ability to process sensory information and generate motor actions at millisecond time scales [20]. In recent years, new theories have emerged that view the brain as an active and adaptive system in which there is a close connection between cognition and action [5]. Instead of viewing cognition as building universal, context independent models of the external world [14, 4], cognition is considered to play an important role in the generation of correct action responses in a context dependent adaptive manner [19]. Accordingly, the modern perspective is to relate cognitive functions with coherent behavior of large number of neural populations [3, 34, 19]. This modern view has been particularly relevant for understanding the binding problem which deals with the question of how does the brain integrate sensory information on object properties (color, shape, ...) to identify the object as a coherent whole [27]. Since many objects in the world are multi-sensory, a coherent representation of the object requires integration of responses across different sensory modalities including in various combinations the haptic, visual, olfactory and auditory properties. It is believed that neural synchrony at millisecond level precision is crucial in implementing such an integration across different cortical regions. Although there has been a growing interest in understanding the role for neural synchrony in cognitive processes involved in normal brain functioning, a number of recent works have also examined the relevance of neural synchronization in various neurological diseases such as epilepsy [21], schizophrenia [24], autism [26] and Alzheimers disease [30].

Sachin S. Talathi
Department of Biomedical Engineering, University of Florida, e-mail: stalathi@bme.ufl.edu

Pramod P. Khargonekar
Department of Electrical and Computer Engineering, University of Florida e-mail: ppk@ufl.edu

Neural synchrony generally refers to the fact that large numbers of heterogeneous interconnected neurons fire in a precisely coordinated manner to generate very distinct oscillations in different frequency bands. A number of theoritcal studies have employed computational models of neurons and their interactions to in order to understand the mechanisms underlying the generation of such synchronized oscillations [7, 1, 12, 33]. While for large neuronal networks, detailed computational simulations is the main approach [38, 36, 35, 2], it is possible to conduct analytical investigations for small networks with the hope that these analytical tools will shed light on synchronized behavior in large neuronal networks [37, 28, 16, 31].

In recent years, there has been much work in the control theory community on consensus in networks of dynamical systems. In particular, the survey paper by Paley et al [23] contains a large list of references on oscillator models and collective action. Indeed, neural synchrony is a form of consensus and collective behavior. The possibility of controlling pathological brain synchrony in neurological diseases such as Parkinson's disease and epilepsy through electrical stimulation, has also spurred interest in the control community to device novel control algorithms, that are based on intrinsic neural populations dynamics [6]. As such, we expect that in the future there will be new research directions at the interface of research efforts by computational neuroscientists and control theorists.

In this paper, our goal is to demonstrate how weak coupling theory and spike time response curves can be used to analyzed patterns of synchrony in a small network of interacting neurons. We present our analysis of phase locked synchronous states emerging in a simple unidirectionally coupled interneuron network (UCIN) comprising of two heterogeneously firing neuron models coupled through a biologically realistic inhibitory synapse. The paper is divided into following sections. Section 2 provides the mathematical background on the neuron models used in the present study and the weak coupling theory of interacting pulse coupled oscillators. In section 3, we analyze patterns of synchrony in the UCIN using weak coupling theory and nonlinear interaction map derived using spike time response curves. Section 4 presents some concluding remarks.

We are very pleased to dedicate this paper to Professor Yutaka Yamamoto on his 60^{th} birthday. One of us (PPK) has had the good fortune and privilege of being friends with him for nearly 30 years, and also collaborated with him in research on sampled-data control and filtering problems. The present paper is loosely connected to signal processing research in that the brain is one of the most remarkable signal processing and understanding machines in existence.

2 Background

In this section, we will briefly describe some background material from computational neuroscience which is relevant for analysis of synchrony in neuronal networks.

2.1 Mathematical Model of Neuronal Dynamics

We model neuronal dynamics following the universally accepted Hodgkin-Huxley formalism [13] (conductance based neuron models [29]). The basic neuron model satisfies the following current-balance equation for the flow of current through the neuronal membrane.

$$C_M \frac{dv(t)}{dt} + I_{na}(t,v(t)) + I_k(t,v(t)) + I_L(v(t)) + I_{dc} = 0 \tag{1}$$

where, t is typically measured in ms, $v(t)$ is the neuronal membrane potential in mV, and $C_M \frac{dv(t)}{dt}$ is the capacitive component of the membrane current, with C_M being the membrane capacitance in μF/cm^2. The current through voltage gated sodium channel is $I_{na}(t,v(t)) = g_{na} m^3(t) h(t) (v(t) - E_{na})$ and the current through the voltage gated potassium channel is $I_k(t,v(t)) = g_k n^4(t)(v(t) - E_k)$. The leak current resulting from passive flow of all other ions through the membrane is modeled through $I_l = g_l(v(t) - E_l)$. Here g_C and E_C (C$\equiv$na,k,l), represent the maximal conductance in mS/cm^2 and the reversal potential for ion channels in mV respectively. The intrinsic firing frequency of each neuron is dependent on the constant current I_{dc} input to each neuron. The variables $X(t) \equiv \{m(t), h(t), n(t)\}$ which represent the fraction of open ion channels, satisfy the following first order kinetic equation

$$\frac{dX(t)}{dt} = \phi(\alpha_X(v(t))(1 - X(t)) - \beta_X(v(t))X(t)) \tag{2}$$

The model parameters are set to those obtained by Wang and Buzsaki (WB) [36] to simulate the dynamics of a fast spiking cortical interneuron. Specifically the functional form for $\alpha_X(V)$ and $\beta_X(V)$ (X$\equiv$m,n,h) are provided in table 1 and the model parameters are (g_{na},g_k,g_l)=(35,9,0.1) mS/cm^2; (E_{na},E_k,E_l)=(50,$-$90,$-$65) mV and $\phi = 5$.

X	$\alpha_X(V)$	$\beta_X(V)$
m	$\frac{0.1(V+35)}{1-e^{-0.1(V+35)}}$	$4e^{-(V+60)/18}$
h	$0.07e^{-(V+58)/20}$	$\frac{1}{1+e^{-0.1(V+28)}}$
n	$\frac{0.01(V+34)}{1-e^{-0.1(V+34)}}$	$0.125e^{-(V+44)/88}$

Table 1 Functions α_X and β_X for the WB neuron model

2.2 Phase for Limit Cycle Oscillators

Following the well known approach due to Winfree [39], Guckenheimer [11] and Ermentrout [9, 7], we will simplify the analysis of neuronal dynamical networks by using transformation to phase variables. In general, the neuron model described in equations 1 and 2 can be written as

$$\frac{dx}{dt} = f(x, \alpha) \tag{3}$$

We will assume that this system has a normally hyperbolic attracting limit cycle $x_0(t)$ with period T_0 which is a function of parameter α such that $x_0(t+T_0) = x_0(t)$. Equation 3 can then be simplified by defining a scalar phase variable $\phi(x_0) \in [0\ 1)$ such that the phase evolution has a simple form $d\phi/dt = 1/T_0$. Thus, with each point on the limit cycle, there is a unique associated phase.

Now consider a point x_* in the basin of attraction of the limit cycle $x_0(t)$. It is then clear that there is a unique phase $\phi_* \in [0\ 1)$ such that the trajectories of dynamical system defined in 3 starting with initial conditions x_* and $x_0(\phi_* T_0)$ converge asymptotically. We define phase of the point x_* to be ϕ_*. The set of points x_* in the basin of attraction with a given phase ϕ_* define an *isochrone* [39]. With the notion of phase defined in the vicinity of the limit cycle through isochrons, the nonlinear system (3) then induces a differential equation for phase in the basin of attraction:

$$\frac{d\phi}{dt} = g(x(t)) \tag{4}$$

It is important to observe that $g(x) = 1/T_0$ if $x \equiv x_0$.

2.3 Weakly Coupled Oscillators

In order to analyze interactions among neurons and the effect of external stimulus, let us now introduce a small periodic force $\varepsilon p(x,t) = \varepsilon p(x,t+P)$ with period P (ε measure the strength of the forcing term) which is in general different from T_0:

$$\dot{x} = f(x) + \varepsilon p(x,t) \tag{5}$$

Using the notion of isochrons defined above, the phase dynamics for equation 5 in the neighborhood of the unperturbed system $x_0(t)$ can now be written as

$$\frac{d\phi(x)}{dt} = \omega_0 + \varepsilon \bigtriangledown_{\mathbf{x}} \phi . p(x,t) \tag{6}$$

For weak coupling $\varepsilon << 1$, the deviation of x from the limit cycle x_0 is negligible, and in the first order approximation we can evaluate the rhs of eq 6 on the limit cycle:

$$\frac{d\phi(x)}{dt} \approx \omega_0 + \varepsilon \bigtriangledown_x \phi . p(x_0,t) \tag{7}$$

On the limit cycle, there is one-one correspondence between the state variable x and the phase ϕ. We therefore have a closed equation for phase:

$$\frac{d\phi}{dt} = \omega_0 + \varepsilon H(\phi,t) \tag{8}$$

where $H(\phi,t) = Z(\phi).p(x_0(\phi),t)$ is unit period function of ϕ and P period function of t referred to as the "averaged" interaction function [9]. The function $Z(\phi) := \bigtriangledown_x \phi$ is purely a function of the oscillator limit cycle and captures the effect of perturbation on the phases. It is commonly referred to as the infinitesimal phase response curve (iPRC) or the linear response function [15]. It can be shown that $Z(\phi)$ is the adjoint eigenfunction for the linearization of the differential equation given in equation 3, about the stable limit cycle $x_0(t)$ [9, 7], which naturally turns out to be a linear periodic system. Recently, a computationally efficient algorithm using properties of this linear periodic system has been proposed in [10].

A special case of the above setup arises when the periodic perturbation εp is the output of another neuron. In this case, $H(\phi,t) = H(\phi,\phi') = Z(\phi).p(\phi,\phi')$, where ϕ' represents the phase variable for the driver neuron. In the case of weak coupling, to the extent that the change in phase ϕ, $d\phi/dt << \omega_0$ over one cycle of unperturbed oscillator, the effective perturbation can be approximated by averaged perturbation over one cycle of the unperturbed oscillator [8],

$$H(\phi,\phi') = \int_0^1 d\theta Z(\phi+\theta).p(\phi+\theta,\phi'+\theta) \tag{9}$$

In case the perturbation is an independent function of the driver and the driven oscillators, i.e., $p(\phi,\phi') \equiv p(\phi').q(\phi)$, equation 9 can be written as a correlation integral

$$H(\phi'-\phi) = \int_0^1 d\theta Z(\theta-(\phi'-\phi)).p(\theta).q(\theta-(\phi'-\phi)) \tag{10}$$

and the phase dynamics of the perturbed oscillator is given by

$$\frac{d\phi}{dt} = \omega_0 + \varepsilon H(\phi'-\phi) \tag{11}$$

3 Analysis of Phase Locked states in a Coupled Neuronal Network

As mentioned in the Introduction, analysis of synchrony in networks of interacting heterogeneous neurons is important for understanding information processing in the brain. Here we present a relatively simple example of two synaptically coupled

WB neurons (see Figure 1a inset). We analyze phase locked states for this special network.

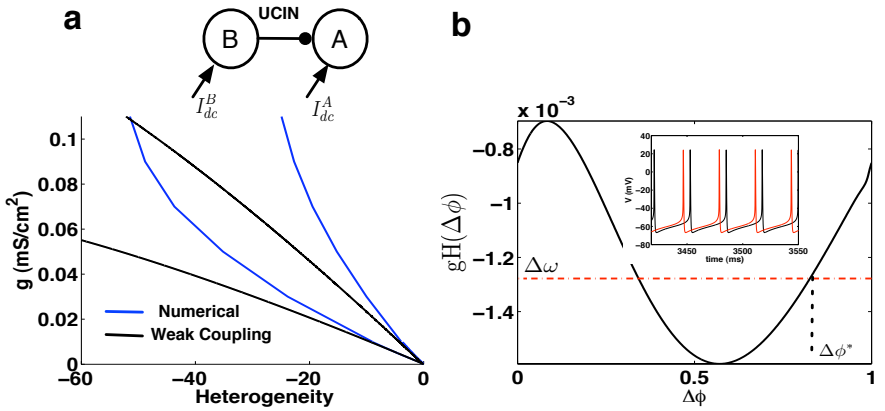

Fig. 1 (a) Arnold tongue for the phase locked states of the unidirectionally coupled interneuron network (UCIN). The region bounded by blue curves represent the Arnold tongue for the UCIN generated through numerical simulation of equations 1,2 and 16 for the two coupled neurons and the synapse. The region bounded by curve in black represents the steady state solution to equation 18 resulting from weak coupling approximation. Inset shows the schematic diagram of the UCIN. (b) Description of procedure to determine steady state fixed point solution to equation 14, for the specific case of heterogeneity H=-4 % resulting from the choice of $I^A_{dc} = 0.5$ μA/cm^2 producing $\omega_A \approx 32.2$ Hz and $I^A_{dc} = 0.48$ μA/cm^2 producing $\omega_B = 30.9$ Hz. The synaptic coupling strength is set at $g = 0.0052$ mS/cm^2. The fixed point $\Delta\phi^*$ corresponds to the stable state solution of equation 14 satisfying conditions in equations 15 and 16 respectively. Inset shows the time series of membrane potential (neuron A in black and neuron B in red) for the particular case considered, when the weak coupling approximation is able to predict the existence of stable phase locked state $\Delta\phi^*$.

3.1 Description of the Network

As shown in Figure 1, WB neuron labelled A fires at intrinsic frequency $\omega_A(I^A_{dc})$ and receives periodic synaptic perturbation from a WB neuron B, which fires with intrinsic frequency $\omega_B(I^B_{dc})$ with $I^B_{dc} \neq I^A_{dc}$. The synaptic coupling is modeled as: $I_s = gs(v_B(t),t)(E_R - v_A(t))$, where g is the strength of synaptic coupling, v_X $\{$X≡A,B$\}$ is the membrane potential, $E_R = -75$ mV is the reversal potential of the synapse and $s(v,t)$ represents the fraction of neurotransmitters bound to the membrane of the post-synaptic cell (neuron A) resulting from the release of these neurotransmitters by neuron B at any given time. It satisfies the following ordinary differential equation

$$\frac{ds(t)}{dt} = \frac{s_0(v_B(t)) - s(t)}{\tau(s_1 - s_0(v_B(t)))} \tag{12}$$

where $s_0(v) = 0.5(1+\tanh(100(v-0.1)))$ and the parameters τ and s_1 are set such that the synaptic rise time $\tau_R = \tau(s_1 - 1) = 0.1$ ms and the synaptic decay time $\tau_D = \tau s_1 = 8$ ms.

3.2 Weak Coupling Approach

If ϕ_A and ϕ_B represent the phase variables of A and B respectively, then we have in the weak coupling limit

$$\begin{aligned} \frac{d\phi_A}{dt} &= \omega_A + gH(\Delta\phi) \\ \frac{d\phi_B}{dt} &= \omega_B \end{aligned} \tag{13}$$

where $H(\Delta\phi) = \int_0^1 Z(\theta - \Delta\phi)s(\theta).(E_R - v(\theta - \Delta\phi))d\theta$ and $\Delta\phi = \phi_B - \phi_A$. The ordinary differential equation for the phase difference $\Delta\phi$ is:

$$\frac{d(\Delta\phi)}{dt} = \Delta\omega - gH(\Delta\phi) \tag{14}$$

where $\Delta\omega = \omega_B - \omega_A$ is the difference in the intrinsic firing rates of the two coupled neurons. *Stable fixed point solution $\Delta\phi^*$ of equation 14 corresponds to the phase locked state of synchronous oscillations between the two coupled neurons in the UCIN.* The fixed point solution satisfies

$$H(\Delta\phi^*) = \Delta\omega/g \tag{15}$$

and the local stability of $\Delta\phi^*$ is guaranteed provided

$$\frac{dH(\Delta\phi)}{d\Delta\phi}|_{\Delta\phi^*} > 0 \tag{16}$$

Two key parameters of the UCIN that influence phase locking behavior are the heterogeneity $\Delta\omega$ and the synaptic coupling strength g. We will now use weak coupling theory to estimate the set of $\{\Delta\omega, g\}$ which corresponds to phase locked synchronous states of UCIN and compare these to the set $\{\Delta\omega, g\}$ which result in phase locked solutions of UCIN using full nonlinear model as described through equations 1, 2 and 12.

Weak coupling theory estimate of $\{\Delta\omega, g\}$ can be obtained by solving equations 15 and 16. Detailed explanation of the this computation is provided in Figure 1b. The resulting domain of $\{\Delta\omega, g\}$ is referred to as the Arnold Tongue [25], which is depicted as the region bounded by black curves in Figure 1a. Arnold tongue for full UCIN is obtained by fixing the firing frequency of neuron A to $\omega_A \approx 32Hz$ and varying the intrinsic firing frequency of neuron B ω_B by changing the dc drive I_{dc}^B on to the neuron B, thereby varying the degree of heterogeneity $H = 100\frac{\omega_B - \omega_A}{\omega_A}$ in the

intrinsic firing rates of the two coupled neurons. The phase locked states correspond to the value of synaptic strength g that result in $< \omega_A > / \omega_B = 1$, where $< \omega_A >$ is the frequency of neuron A when the UCIN settles into steady state. The Arnold tongue so obtained is the region bounded by curves in blue in Figure 1a. We see from Figure 1a that the weak coupling theory based estimate of the Arnold tongue matches that generated through numerical simulations only in the vicinity of $\{0,0\}$. However, there is a significant mismatch for higher values of synaptic strength and heterogeneity in the network.

3.3 Analysis of the Strong Coupling Case

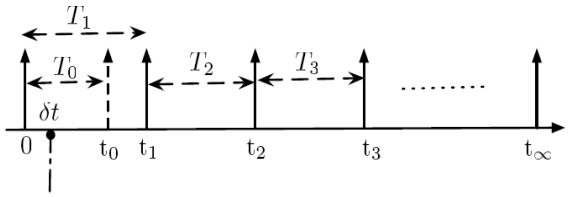

Fig. 2 Schematic diagram representing the effects of external perturbation on the subsequent firing periods of a neuron firing with intrinsic period T_0

In this section, we will introduce the concept of spike time response curves (STRC's), and demonstrate its utility in the analysis of phase locked states in the UCIN in the regions where weak coupling theory fails. In order to motivate the concept of STRC, consider a spontaneously firing neuron with period T_0. At time t following a voltage peak in the firing cycle of a neuron a perturbation, e.g., a depolarizing current pulse is applied. It shifts the time of the next voltage peak as in Figure 2. Let T_j (j=1,2,...) represent the times of j^{th}voltage peak after the perturbation. The quantities $\Phi_{j,\alpha} = \frac{T_0 - T_j}{T_0}$, which measure the shift in the phase of neuron in response to a perturbing stimulus are called the STRC's. The parameter α corresponds to the dependence of STRC on the characteristics of the perturbation input. If the perturbation impulse occurs through a chemical synapse, a case of particular importance to the analysis of the UCIN we consider here, α represents the set of synaptic parameters such as the rise time of the synapse τ_R, the decay time of the synapse τ_D, the synaptic reversal potential E_R and the synaptic coupling strength g. The STRC's can be computed numerically by solving the nonlinear dynamical equations for a given neuron receiving the perturbation and measuring the length of subsequent firing cycles [1]. For the network under consideration, we specifically computed STRC's for an intrinsically firing WB neuron with frequency $\omega \approx 32$ Hz receiving perturbation through an inhibitory synapse with reversal potential $E_R = -75$ mV, $g = 0.15$

mS/cm^2 $\tau_D = 8$ ms, $\tau_R = 0.1$ ms. In Figure 3a, we show the STRC's $\Phi_j(\delta t)$ (j=1,2) as a function of the time δt at which it receives the perturbation.

We will now use these STRC's obtained numerically for different levels of synaptic coupling strengths g to derive a nonlinear map for the evolution of phase difference $\Delta\phi$ between the two coupled neurons in the UCIN. In Figure 3b, we show a schematic diagram of spike times of the two neurons when they are phase locked. Let t_X^n {X≡A,B} be the time of n^{th} spike generated from neurons A and B respectively. Define δ^n to be the time in the n^{th} firing cycle of neuron A when it receives synaptic perturbation from neuron B. If P_A^n represents the length of n^{th} firing cycle of neuron A, then from Figure 3b, we have $P_A^n = t_A^{n+1} - t_A^n = F_A^n + R_A^n$, where $F_A^n = \delta^n + T_A\Phi_2(\delta^{n-1})$ is the entrained firing interval defining the time elapsed between the firing of neuron A at time $t_A^n$and the firing of pre-synaptic neuron B at time t_B^n [22]. In writing this equation, we assume that the oscillator returns back on to the limit cycle in between periodic perturbations. Analysis of phase locked state between oscillators when this condition is not met has been recently performed by [32] and is beyond the scope of this article.The entrained recovery interval defining the time interval between the firing of the pre-synaptic neuron at time t_B^n and the next firing of neuron A at time t_A^{n+1} is then given as $R_A^n = T_A(1 + \Phi_1(\delta^n)) - \delta^n$, which follows from the definition of Φ_1. From Figure 3b, we have

$$T_B = t_B^{n+1} - t_B^n = R_A^n + F_A^{n+1} \tag{17}$$

resulting in the following nonlinear map for the evolution of δ^n

$$\delta^{n+1} = \delta^n + T_B - T_A(1 + \Phi_1(\delta^n) + \Phi_2(\delta^n)) \tag{18}$$

The stable fixed point solution of the nonlinear map given through equation 18 represent the phase locked state of the UCIN. The fixed point δ^* of equation 18 satisfies $1 + \Phi_\infty(\delta^*) = T_B/T_A$, where $\Phi_\infty(x) = \Phi_1(x) + \Phi_2(x)$. The local stability of δ^* requires $0 < \frac{d\Phi_\infty(x)}{dx}|_{x=\delta^*} < 2$. In Figure 3c, the curves shown in black enclose the region of stable fixed point solution to equation 18. We see that the nonlinear map derived from STRC's is successfully able to predict the Arnold tongue corresponding to the phase locked solution for the UCIN even in the strong coupling limit.

4 Discussion

Our primary aim is to develop a research program at the intersection of control, signal processing and computational neuroscience. Here we focused on analysis of synchrony in a simple network of two heterogeneous neurons interacting through a strong inhibitory synapse, the UCIN. Weak coupling theory is general and has proved effective in the analysis of large homogeneous neuronal networks interacting through weak coupling. [18]. It has limitations for the analysis of realistic biological networks [2]. Our analysis of the UCIN specifically demonstrates the limited appli-

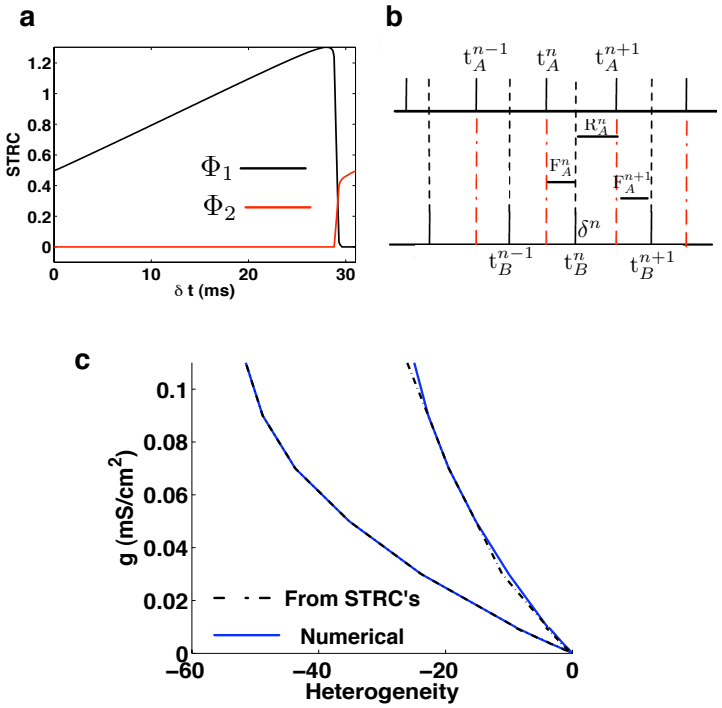

Fig. 3 (a) The STRC's Φ_1 (black line) and Φ_2 (red line) for a WB neuron receiving perturbation through an inhibitory synapse with parameters $E_R = -75$mV, $\tau_D = 8$ ms, and $\tau_R = 0.1$ ms. All higher order STRC's Φ_j (j>2) are zero. (b) Schematic diagram representing spike timing for neurons A and B in the unidirectionally coupled interneuron network (UCIN) when they are phase locked. (c) Arnold tongue for the phase locked states of the UCIN represented by region bounded by blue lines obtained through numerical simulation of equations 1, 2 and 12. The curves in black are obtained as a steady state solution to the nonlinear map in equation 18.

cability of weak coupling theory in predicting synchronous phase locked states of the network. We show that nonlinear maps derived from STRC's can better predict synchronous phase locked states generated by the network in more biologically realistic conditions of moderate to high heterogeneity and strong synaptic interactions.

Understanding the dynamics of large heterogeneous neuronal networks is a major area of research, see e.g., [2]. Analysis of such large networks is primarily done using numerical simulations. Mathematical analysis of small networks (UCIN, for example) has been shown to be fruitful in providing insights into the dynamics of large neuronal networks. In particular, White et al. [37], used a simple two cell network to shed light on two distinct mechanisms which synchrony in large networks can be lost. Similarly, Skinner et al. [28], have shown that coherent states observed in two cell networks in the presence of heterogeneity are preserved in large neuronal networks suggesting that a strategy of analysis on small network dynamics might be a useful way to understand the contribution of biophysical parameters in the gen-

eration of synchronous states in large biological networks. Finally, it is hoped that interdisciplinary efforts will lead to new mathematical analysis techniques that will apply to large heterogeneous neuronal networks.

References

1. C.D. Acker, N. Kopell, and J.A. White. Synchronization of strongly coupled excitatory neurons: relating network behavior to biophysics. *J Comput Neurosci*, 15(1):71–90, 2003.
2. M. Bartos, I. Vida, and P. Jonas. Synaptic mechanisms of synchronized gamma oscillations in inhibitory interneuron networks. *Nat Rev Neurosci*, 8(1):45–56, 2007.
3. R.D. Beer. Dynamical approaches to cognitive science. *Trends Cogn Sci*, 4(3):91–99, 2000.
4. I. Biederman. Recognition-by-components: a theory of human image understanding. *Psychol Rev*, 94(2):115–47, 1987.
5. A. Clark. An embodied cognitive science? *Trends Cogn Sci*, 3(9):345–351, 1999.
6. P. Danzl and J. Moehlis. Spike timing control of oscillatory neuron models using impulsive and quasi-impulsive charge balanced inputs. American Control Conference, 2008.
7. G.B. Ermentrout. Type i membranes, phase resetting curves, and synchrony. *Neural Comput*, 8(5):979–1001, 1996.
8. G.B. Ermentrout and N. Kopell. Frequency plateaus in a chain of weakly coupled oscillators. *SIAM J. Math Anal*, 15:215–237, 1984.
9. G.B. Ermentrout and N. Kopell. Multiple pulse interactions and averaging in systems of coupled neural oscillators. *J Math Biol*, 29:195–217, 1991.
10. W. Govaerts and B. Sautois. Computation of the phase response curve: a direct numerical approach. *Neural Comput*, 18(4):817–847, 2006.
11. J. Guckenheimer and P. Holmes. *Nonlinear Oscillations, Dynamical Systems, and Bifurcations of Vector Fields*. Springer, 2002.
12. D. Hansel, G. Mato, and C. Meunier. Synchrony in excitatory neural networks. *Neural Comput*, 7(2):307–337, 1995.
13. A. Hodgkin and A. Huxley. A quantitative description of membrane current and its application to conduction and excitation in nerve. *J Physiol*, 117:500–544, 1952.
14. D. H. Hubel and T. N. Wiesel. Receptive fields and functional architecture in two nonstriate visual areas (18 and 19) of the cat. *J Neurophysiol*, 28:229–89, 1965.
15. E.M. Izhikevich and G.B. Ermentrout. Phase model. *Scholarpedia*, 3:1487, 2008.
16. H. Jeong and B. Gutkin. Synchrony of neural oscillations controlled by gabaergic reversal potentials. *Neural Comput*, 19:706–729, 2007.
17. E.R. Kandel, J.H. Schwartz, and T.M. Jessel. *Principles of Neural Science*. 2000.
18. Y. Kuramoto. *Collective behavior of coupled oscillators: In Handbook of brain theory and neural networks*. MIT Press, Cambridge MA, 1995.
19. A.B. Markman and E. Dietrich. Extending the classical view of representation. *Trends Cogn Sci*, 4(12):470–475, 2000.
20. S. Molholm, W. Ritter, M.M. Murray, D. C. Javitt, C. E. Schroeder, and J. J. Foxe. Multisensory auditory-visual interactions during early sensory processing in humans: a high-density electrical mapping study. *Brain Res Cogn Brain Res*, 14(1):115–28, Jun 2002.
21. E. Neidermeyer. *Epileptic Seizure Disorders. In Electroencephalography: Basic Principles, Clinical Applications and Related Fields*. Lippincott Williams and Wilkins, 2005.
22. S.A. Oprisan and C.C. Canavier. Stability analysis of ring of pulse coupled oscillators:the effect of phase resetting in the second cycle is important at synchrony and for long pulses. *Differential Equations and Dynamical Systems*, 9:243–258, 2001.
23. D.A. Paley and N.E. Leonard. Oscillator models and collective motion. *IEEE Control Systems Mag*, 27:89–105, 2007.

24. W. A. Phillips and S. M. Silverstein. Convergence of biological and psychological perspectives on cognitive coordination in schizophrenia. *Behav Brain Sci*, 26(1):65–82; discussion 82–137, Feb 2003.
25. A. Pikovsky, M. Rosenblum, and J. Kurths. *Synchronization a universal concept in nonlinear sciences*. Cambridge University Press, UK, 2001.
26. F. Polleux and J. M. Lauder. Toward a developmental neurobiology of autism. *Ment Retard Dev Disabil Res Rev*, 10(4):303–17, 2004.
27. A. L. Roskies. The binding problem. *Neuron*, 24(1):7–9, 111–25, Sep 1999.
28. F. K. Skinner, J. Y. J. Chung, I. Ncube, P. A. Murray, and S. A. Campbell. Using heterogeneity to predict inhibitory network model characteristics. *J Neurophysiol*, 93(4):1898–1907, 2005 Apr.
29. F.K. Skinner. Conductance based models. *Scholarpedia*, 1(11):1408, 2006.
30. C. J. Stam, Y. van der Made, Y. A. L. Pijnenburg, and P. Scheltens. Eeg synchronization in mild cognitive impairment and alzheimer's disease. *Acta Neurol Scand*, 108(2):90–6, Aug 2003.
31. S. S. Talathi, Dong-Uk Hwang, and W. L. Ditto. Spike timing dependent plasticity promotes synchrony of inhibitory networks in the presence of heterogeneity. *J Comput Neurosci*, 25(2):262–281, 2008 Oct.
32. S.S. Talathi, Dong-Uk Hwang, A. Miliotis, P.R. Carney, and W.L. Ditto. Predicting synchrony in heterogeneous pulse coupled oscillators. *Phys Rev E*, In press, 2009.
33. C. Van Vreeswijk, L. F. Abbott, and G. B. Ermentrout. When inhibition not excitation synchronizes neural firing. *J Comput Neurosci*, 1(4):313–321, 1994 Dec.
34. F. Varela, J. P. Lachaux, E. Rodriguez, and J. Martinerie. The brainweb: phase synchronization and large-scale integration. *Nat Rev Neurosci*, 2(4):229–39, Apr 2001.
35. I. Vida, M. Bartos, and P. Jonas. Shunting inhibition improves robustness of gamma oscillations in hippocampal interneuron networks by homogenizing firing rates. *Neuron*, 49(1):107–117, 2006 Jan 5.
36. X. J. Wang and G. Buzsáki. Gamma oscillation by synaptic inhibition in a hippocampal interneuronal network model. *J Neurosci*, 16(20):6402–13, Oct 1996.
37. A. White, C. Chow, J. Ritt, C. Trevino, and N. Kopell. Synchronization and oscillatory dynamics in heterogeneous mutually inhibitory neurons. *J Comput Neurosci*, 5:5–16, 1998.
38. M. A. Whittington, R. D. Traub, and J. G. Jefferys. Synchronized oscillations in interneuron networks driven by metabotropic glutamate receptor activation. *Nature*, 373(6515):612–615, 1995 Feb 16.
39. A. T. Winfree. *The geometry of biological time*. Springer; 2nd edition, 2001.